Impact of 0.35 T Magnetic Field on Dose Calculation for Non-small Cell Lung Cancer Stereotactic Radiotherapy Plans

Jaeman Son[1], Sung Young Lee[1], Chang Heon Choi[1], Jong Min Park[2], Jung-in Kim[1]

[1]Department of Radiation Oncology, Seoul National University Hospital, Seoul, Korea; [2]Department of Radiation Oncology, Seoul National University College of Medicine, Seoul, Korea

ABSTRACT

Background: We investigated the impact of 0.35 T magnetic field on dose calculation for non-small cell lung cancer (NSCLC) stereotactic ablative radiotherapy (SABR) in the ViewRay system (ViewRay Inc.), which features a simultaneous use of magnetic resonance imaging (MRI) to guide radiotherapy for an improved targeting of tumors.

Materials and Methods: Here, we present a comprehensive analysis of the effects induced by the 0.35 T magnetic field on various characteristics of SABR plans including the plan qualities and dose calculation for the planning target volume, organs at risk, and outer/inner shells. Therefore, two SABR plans were set up, one with a 0.35 T magnetic field applied during radiotherapy and another in the absence of the field. The dosimetric parameters were calculated in both cases, and the plan quality indices were evaluated using a Monte Carlo algorithm based on a treatment planning system.

Results and Discussion: Our findings showed no significant impact on dose calculation under the 0.35 T magnetic field for all analyzed parameters. Nonetheless, a significant enhancement in the dose was calculated on the skin surrounding the tumor when the 0.35 T magnetic field was applied during the radiotherapy. This was attributed to the electron return effect, which results from the deviation of the electrons ejected from tissues upon radiation due to Lorentz forces. These returned electrons re-enter the tissues, causing a local dose increase in the calculated dose.

Conclusion: The present study highlights the impact of the 0.35 T magnetic field used for MRI in the ViewRay system for NSCLC SABR treatment, especially on the skin surrounding the tumors.

Keywords: Non-small Cell Lung Cancer, Viewray System, Low Magnetic Field, Dosimetric Parameters

Original Research

Introduction

Non-small cell lung cancer (NSCLC) is a major cause of cancer-related mortality worldwide, with more than 1,000,000 related deaths occurring each year [1–3]. Although surgery is the most representative treatment for NSCLC cases with high mortality rates, it does not constitute a default option for a significant percentage of patients owing to various reasons. In fact, approximately 30% of early-stage NSCLC patients do not have surgery, with 65% of elderly patients older than 75 years [4]. Additionally, patients with

comorbidities, which may increase surgical risk, generally do not undergo surgery [5–7]. Nonetheless, a decision not to undergo surgery can also be due to a patient's perception of prognosis and racial factors. Thus, for patients excluding the surgery option, Stereotactic ablative radiotherapy (SABR) is the alternative route to conventional fractionated radiotherapy [8–10]. SABR is a radiotherapy method with extremely high ablation doses, usually provided in three to eight treatment fractions within 2 weeks, to minimize the toxicity risk induced to normal cells. Many studies have demonstrated that SABR treatment for NSCLC patients achieves better local control, survival rates, and less toxicity, compared to conventional radiotherapy [5, 11, 12]. Nonetheless, the SABR treatment requires a set of logistics including immobilization to prevent patient movements during radiation treatment, treatment plans, and actions to describe tumor movements during radiation delivery, dose distribution for tumors, and steep dose slopes from tumors to surrounding normal tissue [13, 14]. SABR is a method of high-precision radiation therapy with a relatively larger amount of irradiation per fraction than conventional fractionated radiotherapy, which imposes an essential need for highly accurate treatment. The ViewRay system (ViewRay Inc.) provides means to deal with most of the SABR treatment requirements. Magnetic resonance imaging (MRI) is performed in real-time, with a 0.35 T magnetic field, during radiation treatment [15–17]. This enables accurate doses to be delivered to the targeted tumor. However, the low magnetic strength used in ViewRay infers poor image quality. Most importantly, the magnetic field during treatment affects dose calculations, causing dose enhancement or reduction. Raaijmakers et al. [18] reported a reduced build-up distance induced by the magnetic field because it creates an electron trajectory between collisions in the form of curves. In addition, a dose enhancement usually arises due to the electron return effect (ERE) at tissue-air interfaces. Electrons leave the tissue at a certain rate and then deviate from the path by the magnetic field, curve in the air and enter the tissue again, causing a local dose enhancement. Raaijmakers et al. [19] found that ERE increased the dose enhancement by 40% at the beam exit region. This phenomenon affects the dose depositions in the clinical planning stage [19]. Esmaeeli et al. [20] reported the effects of a magnetic field (1.5 or 3.0 T) on dose distribution in breast-cancer plans. Besides, Kim et al. [21] reported the impact of a low magnetic field on dose calculation for partial breast irradiation. In particular, observations on the outside of the body confirmed maximum

dose (D_{max}) showed a 5.0±10.5 Gy dose difference. Moreover, Son et al. [22] evaluated the influence of the magnetic field in the prostate SABR plan. It was reported that D_{max} differs by 1.28±1.08 Gy on the outside of the body, confirming that the magnetic field has an influence at the tissue-air interface, inducing alterations to the dose calculation. The tumors in patients with NSCLC are surrounded by more air, compared to the tumors in patients with partial breast or prostate cancer. Therefore, in this study, we evaluated the effect of a 0.35 T magnetic field used in ViewRay on dose deposition. Clinically relevant dosimetric parameters and plan qualities were analyzed by comparing the presence/absence of a 0.35 T magnetic field for NSCLC SABR plans.

Materials and Methods

1. Patient Selection

Twenty patients who have undergone SABR treatment for NSCLC between January 2014 and February 2022 were selected using ViewRay, retrospectively.

2. Treatment System (ViewRay)

The ViewRay system consists of a radiation therapy technique using three ^{60}Co sources, accompanied by MRI with a 0.35 T magnetic field. The system was equipped with three depleted ^{60}Co heads on a ring-shaped gantry. Each multi-leaf collimator (MLC) used in this system is composed of two leaf banks equipped with a total of 60 equally mounted double-focus leaves (30 on each leaf bank). The leaf width of the MLC was 1.05 cm at the plane of the isocenter at a source to axis distance of 105 cm. Each leaf had a 0.3 mm thickness of tongue and groove on the leading edge and a 0.5 mm thickness on the adjacent sides. The interval gap of MLCs is 0.5 cm with a maximum aperture size of 27.3 cm × 27.3 cm at the isocenter.

3. SABR Plans for Lung Cancer

The treatment plans without main magnetic field (B_0) = 0 T treatment plans that are being compared with the B_0 = 0.35 T plans were not created from scratch. Instead, the B_0 = 0 T plans were recalculated (but not re-optimized) with B_0 = 0.35 T plans to determine the extent to which the 0.35 T magnetic field affects dose depositions. The volume of planning target volumes (PTV) has a range of 3.0 to 41.0 cm³, with an average volume of 15.6 cm³. The isocenter was laterally fixed in order to prevent collision between the bore of the ^{60}Co system and the patient's arms. The dose was calculated with an

radiofrequency coil using a 3 mm calculation grid size. The dose calculation of the ^{60}Co system is achieved based on the Monte Carlo (MC) calculation algorithm developed by the manufacturer (ViewRay Inc.). The dose volume histogram (DVH) was analyzed for dosimetric parameters obtained from the ViewRay system.

4. Statistics Analysis

We used the IBM SPSS version 23.0 statistical software (IBM Co.) for the analysis. We used the paired *t*-test to evaluate the difference in dose deposition with and without a 0.35 T magnetic field. The paired *t*-test compares the means of two results taken from the related targets. The results are presented as the average±standard deviation. Paired *t*-tests and paired-sample comparisons were calculated.

5. Plan Evaluation

We used the DVHs to assess the impact of the 0.35 T magnetic field. The corresponding results were analyzed for the presence/absence of a low magnetic field, respectively. For the PTV, we compared the results of dose for mean dose (D_{mean}), minimum dose (D_{min}), D_{max}, the dose delivered to the 5%, 90%, 95%, and 100% of the volume ($D_{5\%}$, $D_{90\%}$, $D_{95\%}$, and $D_{100\%}$, respectively). For organs at risks (OARs), the dosimetric parameters were compared with D_{max} for the spinal cord; D_{max} for the heart; D_{max} for bronchi; D_{max} and the volume re-

ceiving doses equal to or greater than 40 Gy (V_{40Gy}) for ribs; D_{max} for skin; D_{mean}, the volume receiving doses equal to or greater than 10 Gy (V_{10Gy}), the volume receiving doses equal to or greater than 5 Gy (V_{5Gy}), and the dose delivered to the volume 1,000 cm^3 (D_{1000cm^3}) for the contralateral lung; and D_{mean}, the volume delivered to the 20 Gy (V_{20Gy}), V_{10Gy}, V_{5Gy}, and D_{1000cc} for the ipsilateral lung. We also analyzed D_{mean}, D_{min}, and D_{max} for the inner and outer shells (±3 mm from body surface) in order to evaluate the impact of the magnetic field in the patient surface region. Furthermore, the change in the plan's quality was quantitatively evaluated based on the change in dosimetric parameters. The homogeneity index (HI), conformity index (CI), and target coverage were analyzed to evaluate the plan's qualities. The HI, which quantifies the dose homogeneity in the PTV, was calculated as the ratio of $D_{5\%}$ to $D_{95\%}$ [23]. The CI, which indicates the relationship between isodose distribution and PTV, was calculated as the ratio of the prescription dose delivered volume to the PTV volumes [24]. All plans have a target coverage of 95% for the target volume, receiving 100% of the prescription dose.

Results and Discussion

Fig. 1 shows the comparison results of the dose deposition in the presence/absence of a 0.35 T magnetic field.
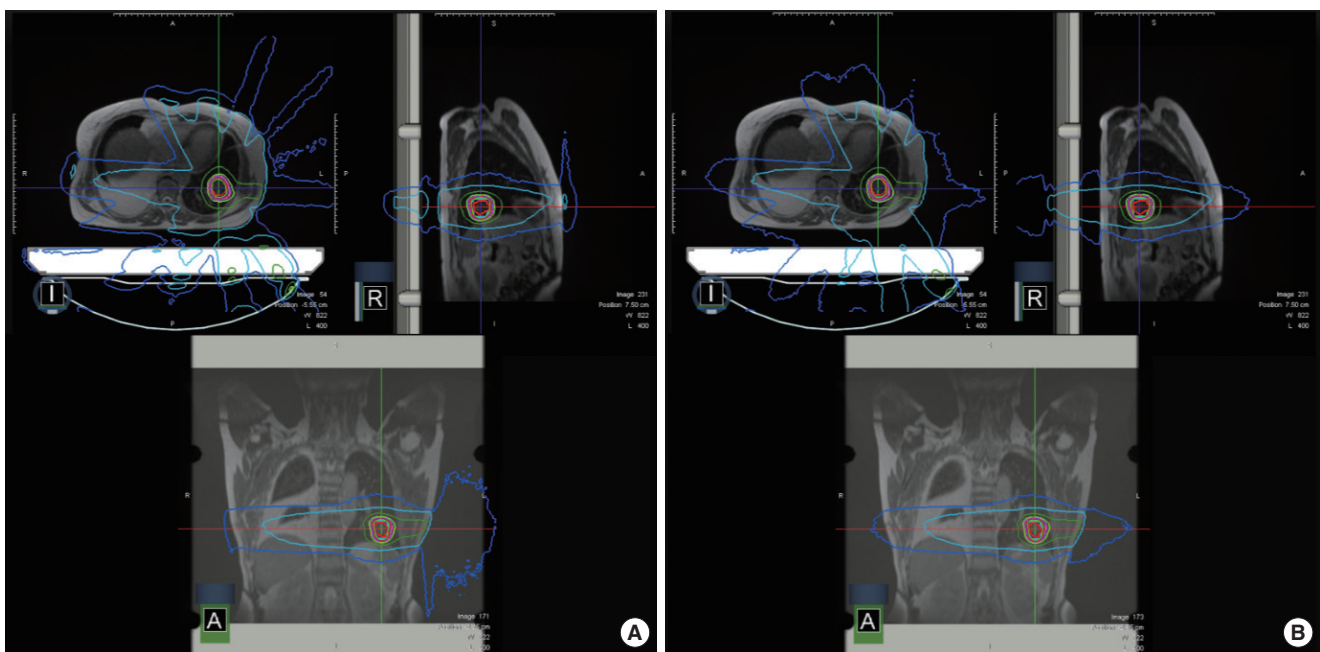

Fig. 1. An example of dose calculation for non-small cell lung cancer stereotactic radiotherapy plan: (A) with a magnetic field ($B_0 = 0.35$ T), (B) without a magnetic field.

Table 1. Planning Target Volume Dosimetric Parameters with/without Magnetic Field

Parameter	With magnetic field	Without magnetic field	Difference value	p-value
D_{mean} (Gy)	56.50±5.41	56.62±5.28	0.21±0.18	0.356
D_{min} (Gy)	51.01±5.37	51.02±5.63	0.48±0.34	0.380
D_{max} (Gy)	60.09±5.67	60.13±5.12	0.58±0.43	0.381
$D_{5\%}$	58.99±5.48	59.16±5.10	0.31±0.30	0.354
$D_{90\%}$	54.38±5.51	54.37±5.57	0.27±0.28	0.377
$D_{95\%}$	53.79±3.52	53.73±5.60	0.28±0.29	0.387
$D_{100\%}$	51.01±5.37	51.02±5.63	0.48±0.34	0.380

Values are presented as mean±standard deviation.
D_{mean}, mean dose; D_{min}, minimum dose; D_{max}, maximum dose; $D_{5\%}$, dose delivered to the 5% of the volume; $D_{90\%}$, dose delivered to the 90% of the volume; $D_{95\%}$, dose delivered to the 95% of the volume; $D_{100\%}$, dose delivered to the 100% of the volume.

Table 2. Plan Quality Indices with/without Magnetic Field

Parameter	With magnetic field	Without magnetic field	p-value
Homogeneity index	1.099±0.052	1.100±0.052	0.479
Conformity index	1.253±0.155	1.282±0.169	0.289
Target coverage	0.946±0.018	0.935±0.049	0.178

Values are presented as mean±standard deviation.

Table 3. Organs at Risk Dosimetric Parameters with/without Magnetic Field

Parameter	With magnetic field	Without magnetic field	Difference value	p-value
Spinal cord				
D_{max} (Gy)	11.10±4.26	11.10±4.33	0.13±0.12	0.499
Heart				
D_{max} (Gy)	19.13±11.09	19.15±11.08	0.21±0.17	0.498
Bronchi				
D_{max} (Gy)	7.03±14.44	6.98±14.44	0.05±0.08	0.497
Ribs				
D_{max} (Gy)	53.25±6.57	52.41±6.20	0.20±0.28	0.402
V_{40Gy} (%)	3.41±3.05	3.60±3.07	0.15±0.45	0.451
Skin				
D_{max} (Gy)	60.09±5.67	59.92±5.42	0.59±0.42	0.462
Contralateral lung				
D_{mean} (Gy)	1.16±0.59	1.13±0.63	0.04±0.13	0.445
V_{10Gy} (%)	2.02±2.56	2.37±2.61	0.01±0.02	0.420
V_{5Gy} (%)	5.21±5.72	4.94±5.74	0.06±0.07	0.447
D_{1000cm^3} (Gy)	0.27±0.11	0.28±0.10	0.01±0.01	0.418
Ipsilateral lung				
D_{mean} (Gy)	6.36±2.86	6.69±3.35	0.72±2.30	0.375
V_{20Gy} (%)	11.58±6.97	11.63±6.92	0.17±0.29	0.493
V_{10Gy} (%)	22.09±10.47	22.07±10.52	0.13±0.15	0.498
V_{5Gy} (%)	30.95±12.76	30.80±12.71	0.22±0.46	0.485
D_{1000cm^3} (Gy)	0.69±0.52	0.67±0.52	0.02±0.02	0.462

Values are presented as mean±standard deviation.
D_{max}, maximum dose; V_{40Gy}, volume receiving doses equal to or greater than 40 Gy; V_{10Gy}, volume receiving doses equal to or greater than 10 Gy; V_{5Gy}, volume receiving doses equal to or greater than 5 Gy; D_{1000cm^3}, dose delivered to the volume 1,000 cm³; Dmean, mean dose; V_{20Gy}, volume receiving doses equal to or greater than 20 Gy.

1. PTV Dose Distribution Difference

The calculated dose deposition for PTV was obtained with/without a 0.35 T magnetic field. The analyzed doses were D_{mean}, D_{min}, D_{max}, $D_{5\%}$, $D_{90\%}$, $D_{95\%}$, and $D_{100\%}$, as listed in Table 1. The average differences in dose depositions between the cases with/without the magnetic field were determined at D_{mean}, D_{min}, and D_{max} as 0.21±0.18 Gy ($p=0.36$), 0.48±0.34 Gy ($p=0.38$), and 0.58±0.43 Gy ($p=0.38$), respectively. At $D_{5\%}$, $D_{90\%}$, $D_{95\%}$, and $D_{100\%}$, the average differences in dose deposition were calculated to be 0.31±0.30 Gy ($p=0.35$), 0.27±0.28 Gy ($p=0.38$), 0.28±0.29 Gy ($p=0.39$), and 0.48±0.34 Gy ($p=0.38$), respectively.

These results show very small differences between the dose calculations (but only one optimization) in the presence and absence of a 0.35 T magnetic field. This clearly indicates that the 0.35 T magnetic field, used for MRI in the ViewRay system, has no significant effect on the dose depositions for the PTV.

2. Plan Qualities Difference

Table 2 summarizes the plan qualities of the NSCLC SABR plans in the presence/absence of a low magnetic field. The results were analyzed for HI, CI, and target coverage. In the presence of a 0.35 T magnetic field, the following results were obtained for these parameters: HI = 1.01±0.05; CI = 1.25± 0.016; and target coverage = 0.95±0.02. When the calculation was performed without the magnetic field, the following results were obtained: HI = 1.10±0.05; CI = 1.28±0.17; and target coverage = 0.94±0.05. For target coverage, the p-value was determined at 0.18 for the presence/absence of a magnetic field. Therefore, the comparison of these indicators clearly indicates that the plan quality is not affected by the presence and absence of the 0.35 T magnetic field.

3. Organs at Risk Dose Distribution Difference

Table 3 presents the average difference for the OARs including the spinal cord, heart, bronchi, ribs, skin, contralateral lung, and ipsilateral lung. The average differences in D_{max} for the spinal cord, heart, and bronchi, were determined as 0.13±0.12 Gy ($p=0.50$), 0.21±0.17 Gy ($p=0.50$), and 0.05± 0.08 Gy ($p=0.50$), respectively. For the ribs, the differences in D_{max} and V_{40Gy} were 0.20±0.28 Gy ($p=0.40$) and 0.15±0.45% ($p=0.45$), respectively. For the opposite lung where the PTV was located, D_{mean} and D_{1000cc} yielded average differences of

Table 4. Inner/Outer Shell Dosimetric Parameters with/without Magnetic Field

Parameter	With magnetic field	Without magnetic field	Difference value	*p*-value
Inner shell				
D_{mean} (Gy)	1.11±0.58	1.13±0.58	0.03±0.02	0.470
D_{min} (Gy)	0.02±0.02	0.06±0.14	0.04±0.13	0.154
D_{max} (Gy)	30.79±4.92	31.15±5.00	0.47±0.33	0.408
Outer shell				
D_{mean} (Gy)	0.86±0.42	0.87±0.40	0.08±0.06	0.452
D_{min} (Gy)	0.02±0.02	0.03±0.05	0.02±0.04	0.152
D_{max} (Gy)	18.74±6.05	21.20±5.49	3.58±2.60	0.047

Values are presented as mean ± standard deviation.
D_{mean}, mean dose; D_{min}, minimum dose; D_{max}, maximum dose.

0.04±0.13 Gy (p=0.45) and 0.01±0.01 Gy (p=0.42), respectively. For V_{10Gy} and V_{5Gy}, the average differences were 0.01± 0.02% (p=0.42) and 0.06±0.07% (p=0.45), respectively. For the ipsilateral lung, the average differences for D_{mean}, D_{1000cc}, V_{20Gy}, V_{10Gy}, and V_{5Gy} were 0.72±2.30 Gy (p=0.38), 0.02±0.02 Gy (p=0.46), 0.17±0.29% (p=0.49), 0.13±0.15% (p=0.50), and 0.22±0.46% (p=0.49), respectively. The very small differences obtained between the values in the presence and absence of the low magnetic field indicate that these conditions do not affect the dosimetric parameters for various OARs.

4. Dose Distribution Difference around the Skin

The dose difference around the skin in the presence/absence of a low magnetic field is shown in Table 4. For the inner shell, the dose differences in terms of D_{mean}, D_{min}, and D_{max} were 0.03±0.02 Gy (p=0.47), 0.04±0.13 Gy (p=0.15), and 0.47±0.33 Gy (p=0.41), respectively. No statistically significant differences were observed for the inner shell. However, for the outer shell, the differences in terms of D_{mean}, D_{min}, and D_{max} were 0.08±0.06 Gy (p=0.45), 0.02±0.04 Gy (p=0.15), and 3.58±2.60 Gy (p=0.05), respectively. This result means that the D_{max} of the outer shell is significantly affected by the presence of the 0.35 T magnetic field.

The impact on the dose deposition of the 0.35 T magnetic field, applied in ViewRay to guide radiation therapy, was analyzed for SABR plans for NSCLC in terms of the variation in dose distributions for PTV, OARs, and outer/inner shells. The effect on plan quality indices (i.e., HI, CI, and target coverage) was also analyzed. For this, two NSCLC SABR plans were designed: one original plan with a 0.35 T magnetic field and another in the absence of the magnetic field. Although no significant differences were observed in PTV, plan qualities, and OARs, results showed a significant increase in doses out-

side the body. This indicates that the ERE induces variations in the dose deposition around the skin in SABR plans for NSCLC.

The MC algorithm based on a treatment planning system (TPS) was employed to evaluate the treatment plans. To use high performance for the optimized simulation of photons, the TPS system applied a variance reduction technique. Dose calculation based on the MC algorithm in the presence/absence of a magnetic field provides geometric information of secondary electrons generated by photons [25]. These electrons can be bent by Lorentz forces and thus have arc-shaped trajectories in water or tissue, causing physical changes such as reduced accumulation, increased doses, and penumbra [26]. In this case, the deviation in dose distribution might have increased in the body. However, Esmaeeli et al. [20] have shown that a dose distribution with an increase or decrease of 7% or 12%, respectively, might occur near the surface. They argued that the increase or decrease in dose to the PTV, internal and contralateral tissues could be reduced because of the magnetic field. In contrast, we have confirmed in our previous studies that low magnetic fields increase the dose, especially near the body surfaces [21, 25]. In the present study, our findings demonstrate that, in the PTV and internal tissues, the dose distribution with magnetic fields did not change compared to the case where condition without the magnetic field was applied for breast and liver cancers [21, 25]. Nonetheless, we report on a slight increase in dose due to the ERE outside the body. In addition, electrons may be more likely to build-up again, especially in air.

These results indicate that further studies are needed on the impact of low magnetic fields for different treatment techniques and sites. In addition, Unity (Elekta) has been developed to allow 6 MV planarization filter free beams to be irradiated to targets, while simultaneously obtaining images using 1.5 T magnetic fields [27]. In the case of a 1.5 T magnetic field, the differences in dose deposition for the PTV, OARs, and skin are greater than those caused by the impact on the 0.35 T magnetic field [28].

Conclusion

This study shows that a 0.35 T magnetic field has an impact on the dose depositions in NSCLC SABR plans. In particular, there was a significant increase in the outer shell dose under the 0.35 T magnetic field due to scatter radiation or the secondary electrons. No significant differences of dose depo-

sitions were identified in the PTV, plan quality, and OARs.

Ethical Statement

This study was approved by the Institutional Review Board of Seoul National University Hospital (approval number: H-2008-200-1155). Written informed consent by the patients was waived due to a retrospective nature of our study.

Author Contribution

Conceptualization: Kim J. Methodology: Choi CH, Park JM. Formal analysis: Lee SY. Funding acquisition: Kim J. Project administration: Kim J. Visualization: Son J. Writing - original draft: Son J. Writing - review & editing: Son J. Approval of final manuscript: all authors.

References

1. Goldstraw P, Ball D, Jett JR, Le Chevalier T, Lim E, Nicholson AG, et al. Non-small-cell lung cancer. Lancet. 2011;378(9804):1727–1740.
2. Ettinger DS, Akerley W, Bepler G, Blum MG, Chang A, Cheney RT, et al. Non-small cell lung cancer. J Natl Compr Canc Netw. 2010;8(7):740–801.
3. Brown S, Banfill K, Aznar MC, Whitehurst P, Faivre Finn C. The evolving role of radiotherapy in non-small cell lung cancer. Br J Radiol. 2019;92(1104):20190524.
4. Palma D, Visser O, Lagerwaard FJ, Belderbos J, Slotman BJ, Senan S. Impact of introducing stereotactic lung radiotherapy for elderly patients with stage I non-small-cell lung cancer: a population-based time-trend analysis. J Clin Oncol. 2010;28(35):5153–5159.
5. Lagerwaard FJ, Verstegen NE, Haasbeek CJ, Slotman BJ, Paul MA, Smit EF, et al. Outcomes of stereotactic ablative radiotherapy in patients with potentially operable stage I non-small cell lung cancer. Int J Radiat Oncol Biol Phys. 2012;83(1):348–353.
6. Le Chevalier T, Arriagada R, Quoix E, Ruffie P, Martin M, Tarayre M, et al. Radiotherapy alone versus combined chemotherapy and radiotherapy in nonresectable non-small-cell lung cancer: first analysis of a randomized trial in 353 patients. J Natl Cancer Inst. 1991;83(6):417–423.
7. Finlayson E, Fan Z, Birkmeyer JD. Outcomes in octogenarians undergoing high-risk cancer operation: a national study. J Am Coll Surg. 2007;205(6):729–734.
8. Solda F, Lodge M, Ashley S, Whitington A, Goldstraw P, Brada M. Stereotactic radiotherapy (SABR) for the treatment of primary non-small cell lung cancer: systematic review and comparison with a surgical cohort. Radiother Oncol. 2013;109(1):1–7.
9. Cao C, D'Amico T, Demmy T, Dunning J, Gossot D, Hansen H, et al. Surgery versus SABR for resectable non-small-cell lung cancer. Lancet Oncol. 2015;16(8):e370–e371.
10. Iyengar P, Westover K, Timmerman RD. Stereotactic ablative radiotherapy (SABR) for non-small cell lung cancer. Semin Respir Crit Care Med. 2013;34(6):845–854.
11. Verstegen NE, Lagerwaard FJ, Haasbeek CJ, Slotman BJ, Senan S. Outcomes of stereotactic ablative radiotherapy following a clinical diagnosis of stage I NSCLC: comparison with a contemporaneous cohort with pathologically proven disease. Radiother Oncol. 2011;101(2):250–254.
12. Abel S, Hasan S, White R, Schumacher L, Finley G, Colonias A, et al. Stereotactic ablative radiotherapy (SABR) in early stage non-small cell lung cancer: comparing survival outcomes in adenocarcinoma and squamous cell carcinoma. Lung Cancer. 2019; 128:127–133.
13. Vlaskou Badra E, Baumgartl M, Fabiano S, Jongen A, Guckenberger M. Stereotactic radiotherapy for early stage non-small cell lung cancer: current standards and ongoing research. Transl Lung Cancer Res. 2021;10(4):1930–1949.
14. Goldsmith C, Gaya A. Stereotactic ablative body radiotherapy (SABR) for primary and secondary lung tumours. Cancer Imaging. 2012;12(2):351–360.
15. Park JM, Park SY, Kim HJ, Wu HG, Carlson J, Kim JI. A comparative planning study for lung SABR between tri-Co-60 magnetic resonance image guided radiation therapy system and volumetric modulated arc therapy. Radiother Oncol. 2016;120(2):279–285.
16. Choi CH, Park SY, Kim JI, Kim JH, Kim K, Carlson J, et al. Quality of tri-Co-60 MR-IGRT treatment plans in comparison with VMAT treatment plans for spine SABR. Br J Radiol. 2017;90(1070): 20160652.
17. Luterstein E, Cao M, Lamb JM, Raldow A, Low D, Steinberg ML, et al. Clinical outcomes using magnetic resonance-guided stereotactic body radiation therapy in patients with locally advanced cholangiocarcinoma. Adv Radiat Oncol. 2019;5(2):189–195.

18. Raaijmakers AJ, Raaymakers BW, Lagendijk JJ. Integrating a MRI scanner with a 6 MV radiotherapy accelerator: dose increase at tissue-air interfaces in a lateral magnetic field due to returning electrons. Phys Med Biol. 2005;50(7):1363–1376.

19. Raaijmakers AJ, Raaymakers BW, Lagendijk JJ. Magnetic-field-induced dose effects in MR-guided radiotherapy systems: dependence on the magnetic field strength. Phys Med Biol. 2008; 53(4):909–923.

20. Esmaeeli AD, Pouladian M, Monfared AS, Mahdavi SR, Moslemi D. Effect of uniform magnetic field on dose distribution in the breast radiotherapy. Int J Radiat Res. 2014;12(2):151–160.

21. Kim JI, Park SY, Lee YH, Shin KH, Wu HG, Park JM. Effect of low magnetic field on dose distribution in the partial-breast irradiation. Prog Med Phys. 2015;26(4):208–214.

22. Son J, An HJ, Choi CH, Chie EK, Kim JH, Park JM, et al. Assessment of dose distributions according to low magnetic field effect for prostate SABR. J Radiat Prot Res. 2019;44(1):26–31.

23. Kataria T, Sharma K, Subramani V, Karrthick KP, Bisht SS. Homogeneity index: an objective tool for assessment of conformal radiation treatments. J Med Phys. 2012;37(4):207–213.

24. Han G, Liu D, Gan H, Denniston KA, Li S, Tan W, et al. Evaluation of the dosimetric feasibility of hippocampal sparing intensity-modulated radiotherapy in patients with locally advanced nasopharyngeal carcinoma. PLoS One. 2014;9(2):e90007.

25. Son J, Chun M, An HJ, Kang SH, Chie EK, Yoon J, et al. Effect of low magnetic field on dose distribution in the SABR plans for liver cancer. Prog Med Phys. 2018;29(2):47–52.

26. Oborn BM, Metcalfe PE, Butson MJ, Rosenfeld AB. Monte Carlo characterization of skin doses in 6 MV transverse field MRI-linac systems: effect of field size, surface orientation, magnetic field strength, and exit bolus. Med Phys. 2010;37(10):5208–5217.

27. Roberts DA, Sandin C, Vesanen PT, Lee H, Hanson IM, Nill S, et al. Machine QA for the Elekta unity system: a report from the Elekta MR-linac consortium. Med Phys. 2021;48(5):e67–e85.

28. Kubota T, Araki F, Ohno T. Comparison of dose distributions between transverse magnetic fields of 0.35 T and 1.5 T for radiotherapy in lung tumor using Monte Carlo calculation. Med Dosim. 2020;45(2):179–185.